

# Discovery and Biocatalytic Application of a PLP-Dependent Amino Acid $\gamma$ -Substitution Enzyme that Catalyzes C-C Bond Formation

Mengbin Chen,<sup>1</sup> Chun-Ting Liu,<sup>1,3</sup> Yi Tang<sup>1,2,\*</sup>

<sup>1</sup>Department of Chemical and Biomolecular Engineering, <sup>2</sup>Department of Chemistry and Biochemistry, University of California Los Angeles, Los Angeles, California 90095, USA. <sup>3</sup>Massachusetts Institute of Technology, Cambridge, Massachusetts 02139, USA.

Supporting Information Placeholder

**ABSTRACT:** Pyridoxal phosphate (PLP)-dependent enzymes can catalyze various transformations of L-amino acids at  $\alpha$ ,  $\beta$  and  $\gamma$  positions. These versatile enzymes are prominently involved in the biosynthesis of nonproteinogenic amino acids as building blocks of natural products, and are attractive biocatalysts. Here, we report the discovery of a two-step enzymatic synthesis of (2*S*, 6*S*)-6-methyl pipecolate **1**, from the biosynthetic pathway of indole alkaloid citrinadin. The key enzyme CndF is PLP-dependent and catalyzes synthesis of (*S*)-2-amino-6-oxoheptanoate **3** that is in equilibrium with the cyclic Schiff base. The second enzyme CndE is a stereoselective imine reductase that gives **1**. Biochemical characterization of CndF showed this enzyme performs  $\gamma$ -elimination of *O*-acetyl L-homoserine to generate the vinylglycine ketimine, which is subjected to nucleophilic attack by acetoacetate to form the new C $\gamma$ -C $\delta$  bond in **3** and complete the  $\gamma$ -substitution reaction. CndF displays substrate promiscuity towards different  $\beta$ -keto carboxylate and esters. Using a recombinant *Aspergillus* strain expressing CndF and CndE, feeding various alkyl- $\beta$ -keto esters led to the biosynthesis of 6-substituted L-pipecolates. The discovery of CndF expands the repertoire of reactions that can be catalyzed by PLP-dependent enzymes.

Nature is remarkable in building and using structurally diverse amino acids.<sup>1,2</sup> Nonproteinogenic amino acids (NAAs), which constitute 96% of the naturally occurring amino acids,<sup>1</sup> are frequently incorporated into small molecules to broaden reactivity and to establish biologically relevant conformers.<sup>3</sup> Peptides that contain NAAs are less susceptible to proteolysis, thereby increasing the half-lives during circulation.<sup>4,5</sup> The usefulness of NAAs have also been extensively explored through incorporation into recombinant proteins in *Escherichia coli*, yeast, and mammalian cells.<sup>6</sup> Because of these features, new methods to efficiently synthesize NAAs have gained significant attention.<sup>7-8</sup>

Parallel to organic synthesis, biocatalysis has been applied in the enantioselective synthesis of NAAs.<sup>9</sup> For example, threonine aldolases can produce  $\beta$ -hydroxy- $\alpha$ -amino acids with complete stereoselectivity at C $\alpha$  positions and moderate stereospecificity at C $\beta$  positions.<sup>10</sup> Aminomutases have been used to convert  $\alpha$ -amino acids to value-added  $\beta$ -amino acids.<sup>11</sup> Enzymes discovered from natural product biosynthetic pathways that catalyze challenging C-H functionalization have been recently used as biocatalysts for NAA synthesis.<sup>12-14</sup> A notable example by Renata and coworkers showed that GriE,  $\alpha$ -ketoglutarate ( $\alpha$ KG)-dependent hydroxylase, can stereospecifically hydroxylate remote  $sp^3$  carbons in a wide range of  $\alpha$ -amino acids at a preparative scale.<sup>13</sup> Chang et al recently identified  $\alpha$ KG-dependent radical halogenases can halogenate unactivated  $sp^3$  carbons of free amino acids.<sup>14</sup> In these examples, the natural functions of the enzymes are to build NAAs for further modification or uptake by nonribosomal peptide synthetases (NRPS).<sup>15-16</sup> Therefore, mining and characterization of new enzymes from secondary metabolism can be fruitful for discovery of new biocatalysts for NAA synthesis.

Pipecolate and derivatives are privileged building blocks frequently used in medicinal chemistry. Pipecolate is present in several FDA approved therapeutics, such as levobupivacaine and nelfinavir (Figure 1).<sup>4</sup> Pipecolate is also found in natural products as highlighted by rapamycin, in which the L-pipecolate is involved in formation of the macrolactam and interactions with FKBP through hydrogen bonding.<sup>17</sup> Altering the L-pipecolate moiety can change the potency of rapamycin derivatives.<sup>18</sup>

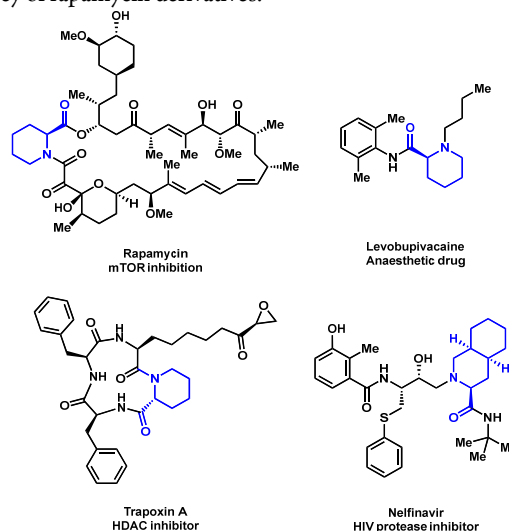
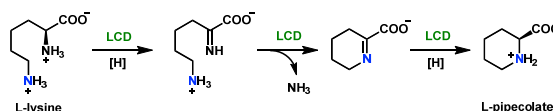


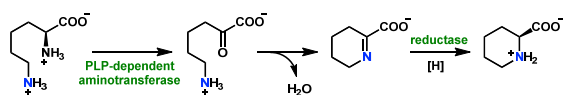
**Figure 1.** Pipecolates are important synthons in medicinal chemistry. Examples of FDA approved drugs containing *N*-heterocyclic amino acids.

Synthetically, pipercolates can be constructed via multiple approaches including aza Diels-Alder cycloaddition between an activated carbodiene and an imine,<sup>19</sup> full reduction of a substituted pipercolate,<sup>20</sup> ring closing metathesis (RCM),<sup>21</sup> or cyclization/reduction of oxo  $\alpha$ -amino acids generated from sulfinimine-mediated asymmetric Strecker synthesis.<sup>22</sup> The last approach resembles one way used by Nature to synthesize unsubstituted L-pipecolate: L-lysine is deaminated to give a cyclic imine, followed by reduction to pipecolate.<sup>23</sup> In rapamycin biosynthesis, a single cyclodeaminase LCD catalyzes both L-lysine deamination and imine reduction (Scheme 1A).<sup>24</sup> In plants, the  $\alpha$ -amine of L-lysine is first converted to ketone followed by Schiff base formation between C $\alpha$  and N $\epsilon$ .<sup>25</sup> Subsequent reduction takes place stereospecifically to give L-pipecolate (Scheme 1B). In fungi, flavin-dependent saccharopine oxidase can generate a C $\epsilon$ -semialdehyde from saccharopine, which can form an imine between N $\alpha$  and C $\epsilon$  (Scheme 1C).<sup>26</sup> This mechanism is analogous to microbial biosynthesis of methylprolines, common building blocks in natural products. Oxygenases can first catalyze remote oxidation of aliphatic amino acids such as L-leucine or L-isoleucine, followed by imine reduction (Scheme 1D).<sup>27-28</sup>

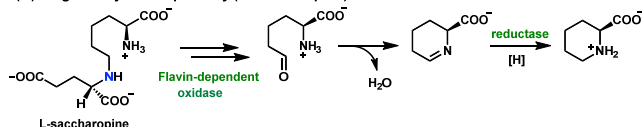
(A) lysine cyclodeaminase (LCD) in rapamycin biosynthesis



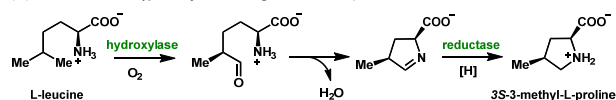
(B) plant biosynthetic pathway (PLP dependent)



(C) fungal biosynthetic pathway (L-saccharopine)



(D) microbial strategy for synthesizing substituted prolines

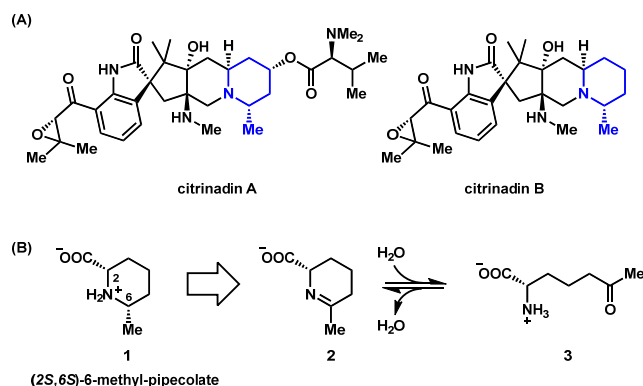


**Scheme 1.** Enzymatic routes to pipecolate and methylated prolines.

Despite their occurrences in drugs such as Nelfinavir, alkyl-substituted pipecolates are extremely rare in natural products. To our knowledge, our recent discovery of 5,5-dimethyl-L-pipecolate in flavunoidine is the only example.<sup>29</sup> Given the linear aliphatic chain in L-lysine and the limited side chain lengths of natural aliphatic amino acids, it is evident that formation of an alkyl-substituted pipecolate via mechanisms shown in Scheme 1 is not possible. Instead, biosynthesis of alkyl-substituted pipecolates will likely involve C-C bond formation between two building blocks to reach the required number of carbons. Uncovering the enzymes that can perform such function can therefore lead to development of biocatalysts for diverse pipecolate synthesis. Here, we reported the discovery of a two-enzyme pathway, including a PLP-dependent  $\gamma$ -substitution enzyme and an imine reductase, to produce (2*S*, 6*S*)-6-methyl pipecolate **1**. We explored the synthetic utility beyond the native substrate to produce a suite of 6-alkyl-pipecolates starting from  $\beta$ -keto esters.

## RESULTS AND DISCUSSIONS

**Citrinadin contains a substituted piperidine.** Active against murine leukemia L1210 cells, citrinadin A and B were isolated from marine *Penicillium citrinum* (Scheme 2).<sup>30-31</sup> Citrinadin A is further modified from citrinadin B with an *N,N*-dimethylvaline ester.<sup>31</sup> Both Citrinadin A and B contain a pentacyclic core structure comprised of spirooxindole and quinolizidine. The complex structures have inspired numerous total synthesis of citrinadin A and B, and the structurally related PF1270A–C.<sup>32-36</sup> Biosynthetically, citrinadin A is a prenylated indole alkaloid, which can be morphed from a monoketopiperazine that is derived from two amino acid building blocks.<sup>37-39</sup> One of the two amino acids is L-tryptophan as evident by the oxindole moiety, while the other becomes part of the quinolizidine, and is predicted to be (2*S*, 6*S*)-6-methyl pipecolate **1** (Scheme 2). Retrobiosynthetically, we propose **1** can be derived from the stereospecific reduction of the Schiff base **2**, analogous to the last step in proline and pipecolate biosynthesis (Scheme 1). **2** is expected to be in equilibrium with the ring opened amino acid (*S*)-2-amino-6-oxoheptanoate **3**, which should be bio-synthesized by dedicated enzymes in the citrinadin biosynthetic cluster from primary metabolites (Scheme 2B).



**Scheme 2.** Citrinadin A and B contains a methylpiperidine that is likely derived from 6-methyl-pipecolate **1**.

The biosynthesis of citrinadin A therefore requires a two-module NRPS that activates and condenses tryptophan and **1**, and at least one dimethylallyl diphosphate transferases (DMAT). The *N,N*-dimethylvaline ester group in citrinadin A is likely installed by an additional single-module NRPS.<sup>29</sup> Using the colocalizations of genes encoding a two-module NRPS and DMAT as requirement, we located a biosynthetic cluster (renamed *cnd*) in several sequenced *Penicillium citrinum* strains (Figure 2A). Among a handful of *P. citrinum* strains that we screened, *P. citrinum* DSM1997 was the only one that produce citrinadin A under laboratory conditions with a titer of 5 mg/L when grown on potato dextrose agar (Figure S2A). To confirm the detected compound is citrinadin A, we performed large-scale culturing of *P. citrinum* DSM1997, purified the compound and verified its structure by NMR analysis (Table S1-2, Figures S13-S14). Next, the *cndA* gene encoding the NRPS was deleted by homologous recombination from the genome to generate *P. citrinum*  $\Delta$ *cndA* (Figure S2B). Metabolic analysis of *P. citrinum*  $\Delta$ *cndA* showed that citrinadin A production was completely abolished (Figure S2), confirming the *cnd* cluster is responsible for citrinadin biosynthesis.

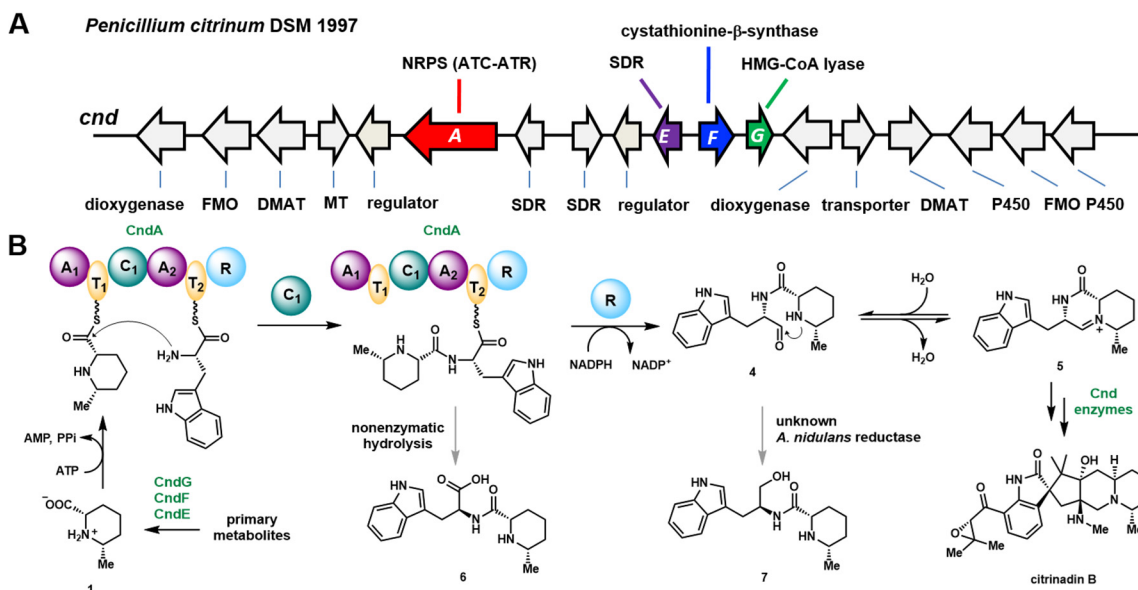


**Figure 2.** Biosynthesis of citrinadin by *Penicillium citrinum* DSM 1997. **(A)** The identified *cnd* gene cluster. The four enzymes that are studied here are colored. Abbreviations: FMO: flavin-dependent monooxygenase; DMAT: dimethylallyltransferases; MT: methyltransferase; SDR: short-chain dehydrogenase/reductase; NRPS: nonribosomal peptide synthetase (A: adenylation; C: condensation; T: thiolation; R: reductase); **(B)** Proposed early steps of citrinadin biosynthesis involves the NRPS CndA and (2*S*,6*S*)-6-methyl-pipecolate **1**.

**Identification of *cnd* biosynthetic cluster.** Since **1** is not a known metabolite, we reasoned enzymes responsible for its biosynthesis are encoded in *cnd* cluster. Through comparative analysis of *cnd* and known gene clusters of other related indole alkaloids that do not incorporate **1**, such as notoamide B and taichuanamide A (Figure S3),<sup>37</sup> a set of *cnd* genes (*cndE-cndG*) that are uniquely present in *cnd* cluster were identified and highlighted in Figure 2A. Basic local alignment search tool (BLAST) searches using CndE as a query revealed that it belongs to short-chain dehydrogenase/reductase (SDR) family. Considering that the final steps in L-proline and L-pipecolate biosynthesis both require reduction of cyclized imine by imine reductases (Scheme 1), we reason that CndE may play a similar role in biosynthesis of **1**.<sup>23, 27-28</sup> The remaining two unique enzymes encoded in the cluster are a pyridoxal phosphate (PLP)-dependent enzyme CndF, and a putative HMG-CoA lyase CndG.<sup>40</sup> The closest known homologue of CndF is PLP-dependent cystathionine- $\gamma$ -synthase (CGS), with a sequence identity of 36%.<sup>41-42</sup> In fungi, CGS catalyzes the  $\gamma$ -elimination of *O*-acetyl homoserine **9** to give a vinylglycine ketimine.<sup>43</sup> The nucleophilic thiolate of cysteine can subsequently attacks C $_7$  atom to form a new C-S bond.<sup>44</sup> We reasoned that CndF may catalyze C-C bond formation between vinylglycine and a three-carbon precursor in a  $\gamma$ -substitution reaction to give (2*S*)-2-amino-6-oxoheptanoate **3** (Scheme 2). If so, CndF would be the first example of a  $\gamma$ -substitution, PLP-dependent enzyme that catalyzes C-C bond formation.

To determine whether **1** is a building block of citrinadins, we heterologously expressed CndA in *Aspergillus nidulans* A1145  $\Delta$ EM.<sup>45</sup> Expressing *cndA* alone did not lead to new metabolites, indicating possible lack of a specific amino acid substrate. Feeding commercially available ( $\pm$ )-*cis*-6-methyl pipecolate, which contain both (2*S*,6*S*) and (2*R*,6*R*) enantiomers, to the *cndA* expression strain led to the production of two new compounds **6** and **7** (Figure 3, vii). NMR characterization revealed **6** and **7** are dipeptides derived from tryptophan and **1** (Tables S5 and S6, Figures S26-S35). Therefore, the exogenously supplied pipecolate is recognized by the NRPS and is

incorporated into the dipeptide (Figure 2). Both compounds are proposed to be off-pathway shunt products that are related to the on-pathway intermediate monoketopiperazine **5**. Formation of the carboxylic acid **6** can be a result of nonenzymatic hydrolysis of dipeptidyl-*S*-PCP from the peptide carrier protein (T<sub>2</sub>) domain of CndA, prior to reductive release as the aldehyde **4** by the R domain (Figure 2B). A sluggish R domain in the heterologous host *A. nidulans* can lead to nonenzymatic hydrolysis of the thioester bond to offload **6**. On the other hand, once released, **4** is in equilibrium with the monoketopiperazine **5**, in which the amide bond is in a less favorable *cis* configuration.<sup>46</sup> In the absence of downstream enzymes that can process **5** to more advanced intermediates, the aldehyde of **4** can be further reduced to the alcohol **7** by endogenous reductases as a detoxification mechanism (Figure 2B).<sup>47</sup>

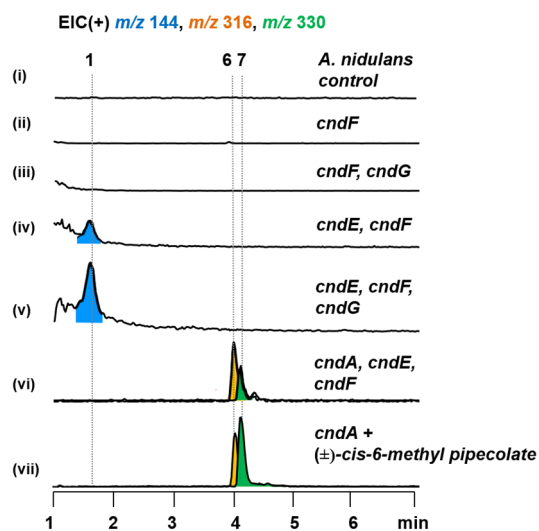


**Figure 3.** Heterologous expression in *A. nidulans* established that CndE and CndF are necessary and sufficient for the formation of **1**.

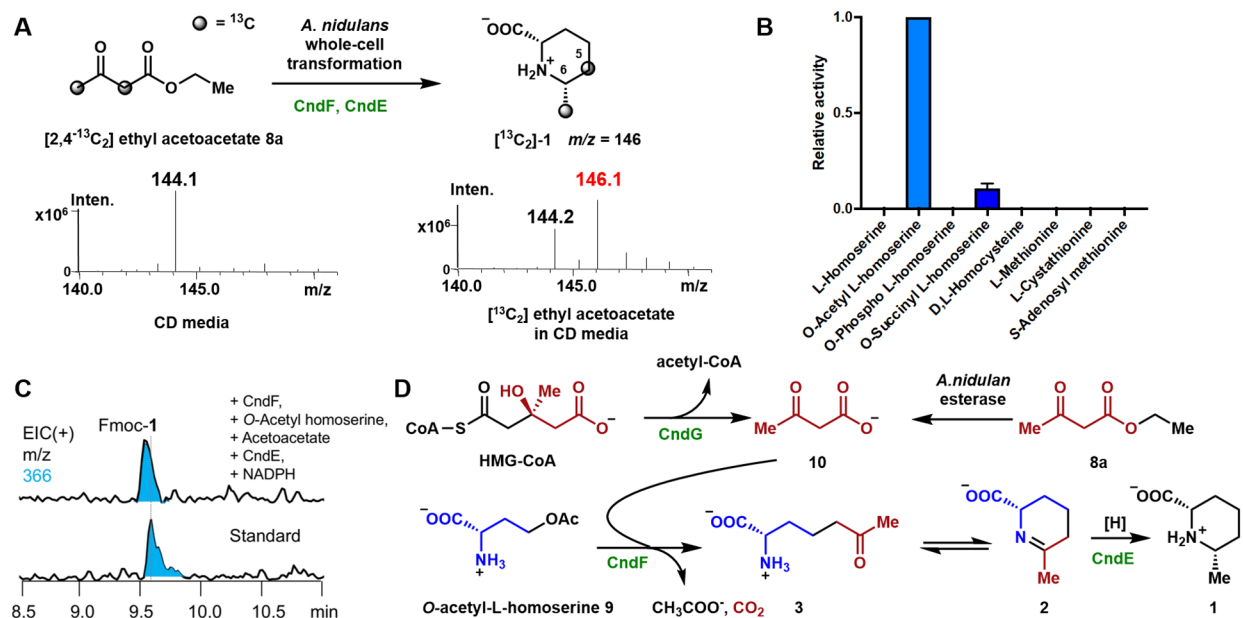


**Figure 4.** CndF and CndE catalyze tandem reactions to yield **1**. (A) Acetoacetate is the precursor to **1**. (B) *In vitro* characterization of CndF revealed that *O*-acetyl-L-homoserine is the preferred amino acid substrate. (C) *In vitro* reconstitution of activities of CndF and CndE to give **1**. (D) Proposed biosynthetic pathway to **1**.

**Determination of the biosynthetic enzymes responsible for producing 1.** To identify the enzymes required to biosynthesize **1** and test the hypothesis that the PLP-dependent CndF catalyzes a C-C bond forming reaction, we reconstituted the activities of CndE, CndF and CndG in *A. nidulans*. Expression of *cndF* alone or with *cndG* did not yield any new product compared to control (Figure 3, i-iii). Co-expression of *cndE* and *cndF* led to formation of a new product with a  $m/z=144$  ( $[M+H]^+$ ) (Figure 3, iv) that agrees with the molecular weight of **1**. We purified the compound with a titer of 5 mg/L and confirmed the structure to be that of **1** by NMR (Table S3, Figures S15-S20). NOESY analysis showed that 2-carboxylate and 6-methyl substituents in **1** are in a *cis* configuration. Purified **1** was derivatized with Marfey's reagent,<sup>48</sup> and the product profile was compared with that of derivatized ( $\pm$ )-*cis*-6-methyl pipecolate (Figure S4). Derivatized **1** elutes as a single peak, whereas the derivatized ( $\pm$ )-*cis*-6-methyl pipecolate elutes as two separate peaks (Figure S4). This demonstrates that **1** is a single enantiomer. Based on the total synthesis and stereochemical assignment of the quinolizidine methyl group in citrinadin to be in *S* configuration,<sup>33-34</sup> we suggest the C6-methyl group in **1** is also in *S* configuration. Hence the structure of **1** is assigned to be (2*S*,6*S*)-6-methyl-pipecolate. This result shows that *cndE* and *cndF* are necessary and sufficient to produce **1**. Expression of *cndE* and *cndF* in the presence of *cndA* led to the production of **6** and **7** (Figure 3, vi), which is consistent with the feeding study with ( $\pm$ )-*cis*-6-methyl pipecolate.

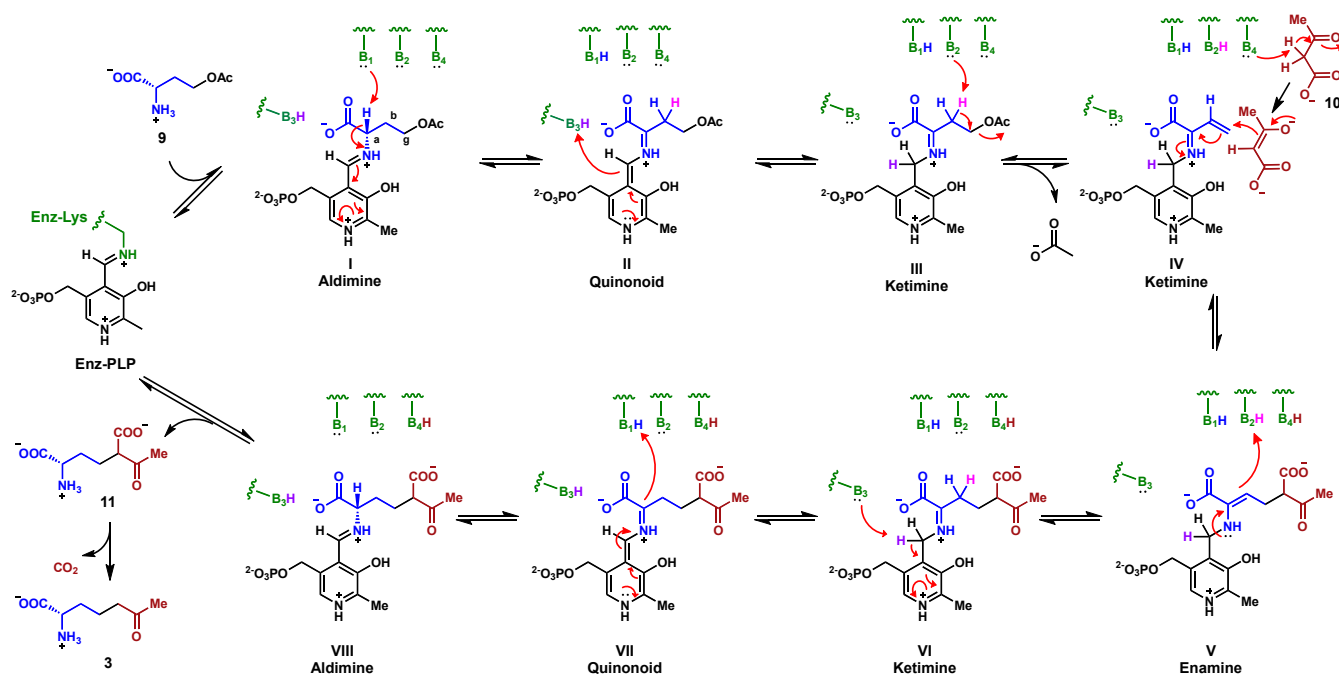
When *cndG* encoding a predicted HMG-CoA lyase was co-expressed in the strain expressing CndE and CndF, the titer of **1** increased by approximately 3-fold (Figure 3, v) to ~15 mg/L, suggesting the activity of CndG increases the availability of precursors to **1**. CndG shows >60% sequence identity with fungal HMG-CoA lyases, which indicates CndG is likely to catalyze the same reaction: the cleavage of HMG-CoA into acetyl-CoA and acetoacetate **10** (Figure 4D).<sup>40</sup> The product **10** could therefore be the three-carbon building block that is used by CndF in constructing **1**. Although extensive efforts were made to obtain cDNA of *cndG* from the native producer, we found that *cndG* remained silent under the citrinadin producing

conditions tested in the lab. Suppression of *ofcndG* expression may be due to sufficient cytosolic concentration of acetoacetate through primary metabolism to maintain the production of citrinadin.

To verify **1** is derived from acetoacetate **10**, we supplied [2,4-<sup>13</sup>C<sub>2</sub>] ethyl acetoacetate **8a** to *A. nidulans* expressing *cndE* and *cndF*. We reasoned the ethyl ester of **8a** may be hydrolyzed by an endogenous esterase to give **10**. As a result of feeding, an increase of 2 mu in MWT of **1** was detected by mass spectrometry (Figure 4A). This indicates both <sup>13</sup>C atoms of **8a** were incorporated into **1**. We purified this labeled compound and NMR analysis revealed that carbon atoms at C5 and the C6-methyl group are isotopically labeled (Figure 4A, Table S4, Figures S21-25). Based on differences in reactivities, we assigned C5 of **1** to correspond to the more nucleophilic C $\alpha$  atom of **8a**, while C6-methyl to correspond to the terminal C $\gamma$  of **8a**. C-C bond formation thus occurs between C $\gamma$  (C4 in **1**) and C $\delta$  (C5 in **1**) to forge **3**, the precursor of **1** (Figure 4D). This agrees with our hypothesis that PLP-dependent enzyme CndF catalyzes C-C bond formation between two smaller precursors.

**CndF is a PLP-dependent  $\gamma$ -substitution enzyme that catalyzes C-C bond formation.** Having established **10** is a building block of **1**, we next sought to elucidate the mechanism of CndF. Since CndF is proposed to catalyze a  $\gamma$ -substitution reaction via a PLP-dependent mechanism, the first substrate must be an amino acid with a good leaving group at C $\gamma$  position. To identify the amino acid substrate of CndF, we heterologously expressed and purified it from *Escherichia coli* with 40  $\mu$ M PLP supplemented in all purification buffers. To confirm that CndF binds PLP, we used UV-vis spectrophotometer to examine to absorbance profile. A characteristic absorption was observed at 420 nm for the purified enzyme, indicating the formation of internal aldimine between PLP and a lysine residue in the active site (Figure S5).<sup>49</sup> Extensive dialysis of CndF in the presence of hydroxylamine eliminated the absorbance peak at 420 nm, indicating the enzyme has been converted to the *apo* form (Figure S5).





**Scheme 3.** Proposed mechanism of CndF in catalyzing the  $\gamma$ -substitution reactions to yield **3**.

Next, we tested a panel of amino acids, including *L*-homoserine, *O*-acetyl-*L*-homoserine **9**, *O*-phospho-*L*-homoserine, *O*-succinyl-*L*-homoserine, *L*-homocysteine, *L*-cystathionine, and *S*-adenosyl-*L*-methionine (SAM), as substrates of CndF in the  $\gamma$ -substitution reaction. *In vitro* reactions of *holo*-CndF were carried out in the presence of **10**. To facilitate product detection of **2** (in equilibrium with **3**) by LC-MS, we used *o*-aminobenzaldehyde (*o*-AB) to derivatize the cyclic imine **2** into the dihydroquinazolinium complex that has a distinct absorbance at 440 nm (Figure S6) and a  $m/z$  of 245. The assays showed that **9** displayed the highest activity among all substrates (Figure 4B), and is therefore the most likely natural substrate for CndF. The only other substrate that supported the formation of **2** was *O*-succinyl-*L*-homoserine.

The proposed mechanism of CndF is shown in Scheme 3. In the first step of the reaction following formation of the external aldimine (**I**) between PLP and **9**, PLP serves as an electron sink to delocalize the negative charge generated by the initial deprotonation event at  $C_\alpha$  position of **9** to give quinonoid (**II**). Divalent metal ions are known to promote electron displacement as a way to stabilize the  $C_\alpha$  carbanion and accelerate catalysis.<sup>50</sup> We carried out *in vitro* enzymatic reactions of CndF in the presence of different divalent metal ions, and found that  $\text{Co}^{2+}$  expedites the reaction most (Figure S7).<sup>50</sup> The remaining steps of  $\gamma$ -elimination and substitution by CndF are analogous to that of cystathionine  $\gamma$ -synthase.<sup>44</sup> Protonation of **II** gives the ketimine (**III**), which can undergo  $C_\beta$  proton abstraction and expulsion of the acetyl group to yield the PLP-bound ketimine form of vinylglycine (**IV**). Next, the acidic proton at  $C_\alpha$  position of acetoacetate is abstracted and the resulting enolate attacks the electrophilic **IV** to form an enamine adduct (**V**). Reprotonation of  $C_\beta$  forms the ketimine (**VI**), followed by quinonoid (**VII**) formation and  $C_\alpha$  protonation to arrive at the new external aldimine (**VIII**). Release of the adduct **11** as product regenerates the internal enzyme-PLP aldimine. The  $\beta$ -carboxylate of **11** can readily undergo decarboxylation to arrive at the desired ketone **3**.<sup>51</sup> While the C-C bond

formation step (**IV**  $\rightarrow$  **V**) may also be initiated through the decarboxylation of **10**, our data below with  $\beta$ -keto ethyl esters suggest the decarboxylation can take place after C-C bond formation. Although decarboxylation is depicted to occur after product release in Scheme 3, we cannot exclude that from taking place during the later catalytic steps of CndF (**V**  $\rightarrow$  **VIII**).

**CndF is a unique PLP-Dependent enzyme.** PLP-dependent enzymes are essential in all kingdoms of life to catalyze many reactions in metabolism, and arguably represent the most versatile biocatalysts.<sup>42</sup> The PLP cofactor enables chemical transformations on amino acids that are otherwise difficult to perform, including transamination, decarboxylation,  $\beta/\gamma$  elimination and substitution, etc.<sup>41</sup> Recently, oxidase activities were also identified in PLP-dependent enzymes.<sup>52</sup> The mechanism of CndF reported here is distinct from known PLP-dependent,  $\gamma$ -substitution enzymes by catalyzing a C-C bond formation between the vinylglycine ketimine and the nucleophilic  $C_\alpha$  in **10**. The closest examples to CndF are cystathionine- $\gamma$ -synthase and LolC found in the loline biosynthetic pathway, which catalyze C-S and a proposed C-N bond formation using the vinylglycine ketimine as electrophile, respectively.<sup>42, 44, 53</sup> Other known C-C bond forming PLP-dependent enzymes, such as UstD in ustiloxin B biosynthesis, can perform  $\beta$ -substitutions using an enamine-PLP as a nucleophile.<sup>42, 54</sup> Threonine aldolases and  $\delta$ -aminolevulinate synthase, which are PLP-dependent enzymes, catalyze C-C bond formation at  $\alpha$ -position of glycine using the nucleophilic glycylic-quinonoid.<sup>10</sup> Our recent discovery of bi-functional FlvA is proposed to be mechanistically similar to CndF, although biochemical validation is still pending.<sup>29</sup>

Searches of the nonredundant protein database in the National Center for Biotechnology Information (NCBI) for CndF homologues revealed numerous candidates across filamentous fungi. None of these homologues have known functions, implicating the untapped functional diversity of these enzymes. Phylogenetic analysis showed that the closest homologues to CndF are co-clustered with other biosynthetic enzymes (Figure S8-9). One group of these

clusters are highly conserved across several *Aspergillus* spp. and all contain a NRPS-independent siderophore (NIS) synthetase, while other cluster contains a single-module NRPS (Figure S9). It is likely that these PLP-dependent enzymes also provide NAAs for downstream incorporation in a secondary metabolite.

**CndE is an imine reductase.** To probe the role of the SDR homolog CndE in reducing **2** to **1**, we carried out combined enzymatic reactions *in vitro*. Purified CndE and CndF (28  $\mu$ M each final concentration) were incubated with **9** (1 mM), **10** (1 mM), NADPH (1 mM), and Co(NO<sub>3</sub>)<sub>2</sub> (2.5 mM) in 50 mM phosphate buffer (pH 6.5) for 1 hour at room temperature. Subsequently, the reaction mix was derivatized with Fmoc-Cl and analyzed by LC-MS. The Fmoc-derivatized product eluted at the same time as Fmoc-**1** (Figure 4C). Formation of **1** is not detected in the absence of CndE or NADPH. Together with earlier chiral derivatization result showing that **1** is a

single enantiomer, these data established **2** that can be stereoselectively reduced to **1** with *S*-configuration at C6 by CndE.

**CndF can synthesize enamines with  $\beta$ -keto esters.** Having verified the activity of CndF, we next probed the substrate scope of CndF by varying the structures of  $\beta$ -keto nucleophile (Figure 5). We chose the ethyl esters **8** as substrates because very few  $\beta$ -keto acids are commercially available due to spontaneous  $\beta$ -decarboxylation. Substrates with different sizes at R<sub>1</sub>, as well as those containing cyclic  $\beta$ -ketones are tested in the assay. We used LCMS to monitor appearance of new products, as well as quantifying the consumption of substrates (Figure S8). If **8** can be recognized by CndF and can form a C-C bond with the vinylglycine ketimine **IV**, then adduct **12** and the cyclized Schiff base are expected to be products. If the  $\alpha$ -position of **8** is not substituted (R<sub>2</sub>=H), the Schiff base is expected to tautomerize and form the stable enamine **13** (Figure 5).

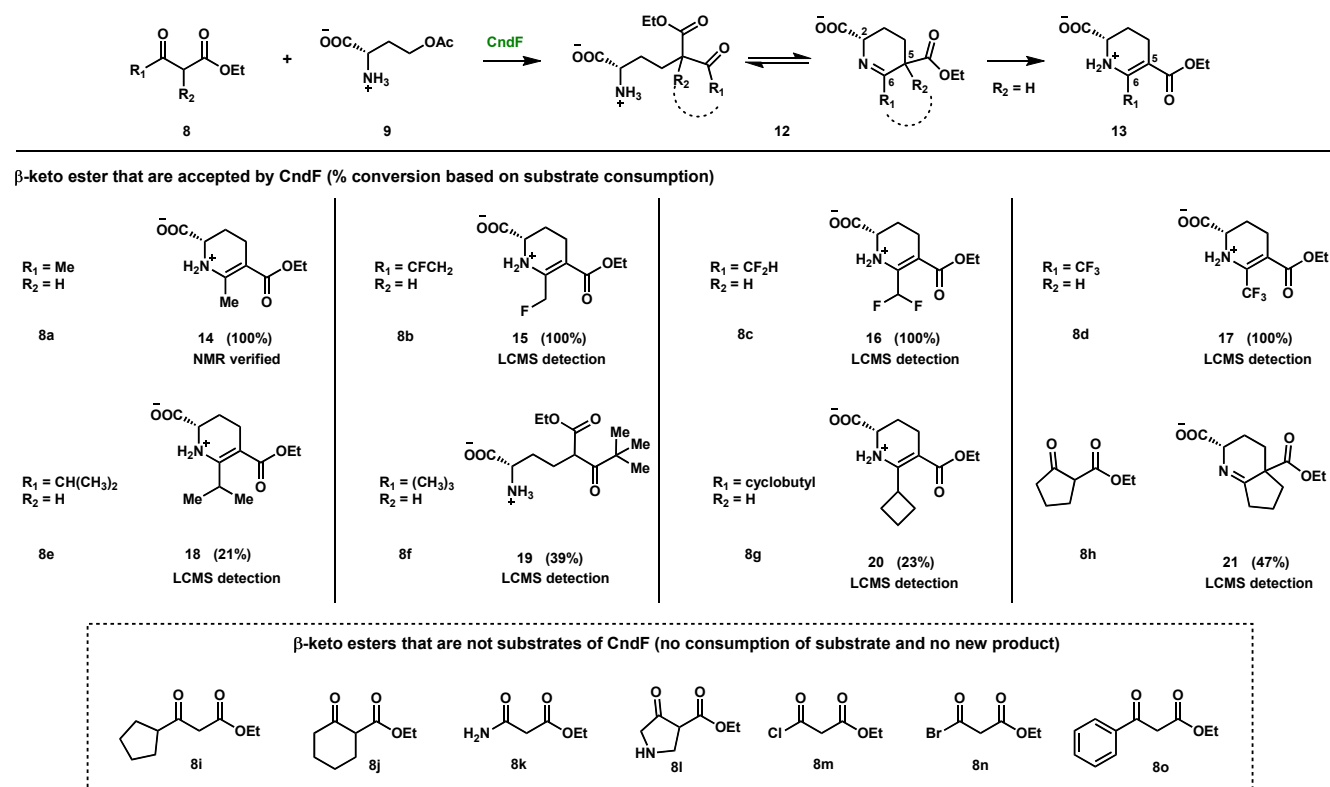


**Figure 5. In vitro assay of  $\beta$ -keto esters with CndF.**

We first tested **8a** in the *in vitro* assay to determine if ethyl esters can be accepted as nucleophiles without being hydrolyzed to the carboxylate. Surprisingly, **8a** can be efficiently converted to a new product **14**, with nearly complete consumption of **8a** (Figure S10A). To produce sufficient amount of **14** for structural determination, we transformed *E. coli* with a plasmid harboring homoserine *O*-acetyltransferase (HAT) and CndF. Overexpression of HAT increases the intracellular levels of **9** for the biotransformation. In addition, **8a** does not undergo hydrolysis readily in *E. coli* due to the absence of the esterase that is presumably present in *A. nidulans*. Feeding L-homoserine (10 mM final concentration) and ethyl acetoacetate **8a** (10 mM final concentration) to *E. coli* culture after IPTG-induced protein expression led to the production of **14** at 30 mg/L after 6 hours. The compound was purified and the structure was solved by NMR to be the enamine shown in Figure 5 (Table S8, Figures S36-S40). The  $\lambda_{\text{max}}$  of **14** at 286 nm is also consistent with reported enamine

absorbance (Figure S10A).<sup>55</sup> Formation of enamine **14** confirms the cyclic Schiff base **12** to be the product of CndF. Coexpression of CndE in *E. coli* did not reduce **14**. This can be attributed to the more stringent substrate specificity of CndE against bulky, C5-substituted cyclic imines. The production of enamine ester **14** also provides mechanistic insight of CndF. In proposing a mechanism for CndF using **10** as the nucleophile, we did not know if decarboxylation is required for enolate formation. Conversion of **8a** to **14** indicates C-C bond formation by CndF does not require acetoacetate decarboxylation to drive enolate formation. Therefore, the presence of a general base (B<sub>4</sub> in Scheme 3) to abstract C $\alpha$  proton is required to form the enolate.

4-Mono-, di-, tri-fluoro ethyl acetoacetate (**8b-d**) can all be converted into new products **15-17** based on LCMS analysis, with full consumption of substrates (Figure S10B-D). Increasing the sizes of

$R_1$  substituent in **8e-g** led to decrease in substrate conversions, although product (**18-20**) formation can still be clearly detected by LCMS (Figure S10E-G). When the *tert*-butyl substrate **8f** was used, only the mass of the uncyclized ketone **19** can be detected (Figure S10F). Formation of the cyclic Schiff base may be impeded by steric hindrances caused by two bulky substituents surrounding the ketone. Further increasing the sizes of  $R_1$  substituent to **8i** and **8o** abolished conversion by CndF, indicating the cyclobutane  $\beta$ -keto ethyl ester **8g** is at the size limit of the CndF active site available for the nucleophile. Surprisingly, we observed ~50% consumption of the cyclopentanone-containing substrate **8h**, and the emergence of a product that matches the expected molecular weight of **21** (Figure S10H). NMR evidence for cyclopentanone incorporation into pipercolate is demonstrated in the next section (see **27**). This result indicates that CndF not only tolerates ethyl esters and  $R_1$  substitutions, but also allows the  $R_2$  position to be substituted. No product can be detected from ethyl 2-cyclohexanone-1-carboxylate **8j**, likely due to the increased size from **8h**. We also tested *N*-containing  $R_1$  variants such as **8k** and **8l**, neither of which was consumed by the enzyme. The substitution of  $-\text{NH}_2$  at  $R_1$  position in **8k** increases pKa of  $\text{C}_\alpha$  proton by 5 units and significantly reduces the nucleophilicity of the enolate. The amine in **8i** is protonated under assay conditions and may prevent binding in a presumably hydrophobic pocket in CndF that binds  $R_1$ , which may also explain the lack of reactivity of **8k**. Halogenated substituents **8m** and **8n** are also not recognized and may covalently inactivate CndF.<sup>56</sup>

**A microbial platform to produce (2*S*, 6*S*)-6-alkyl pipercolate.** The above data showed that CndF has considerable substrate promiscuity to form adducts between vinylglycine and different nucleophiles. However, the use of  $\beta$ -keto ethyl esters *in vitro* or in *E. coli* limits the utility of the enzyme to make alkyl-pipercolate derivatives, due to the inability of CndE to reduce the ester product **12**. The incorporation of [2,4-<sup>13</sup>C<sub>2</sub>]-**8a** to **1** using *A. nidulans* as a host showed that the ethyl esters can be converted to the corresponding  $\beta$ -keto carboxylates *in cellulo* by endogenous esterase and lipases (Figure 4A).<sup>57</sup> Encouraged by this finding, we explored the use of *A. nidulans* expressing CndF and CndE as a biotransformation host to convert various  $\beta$ -keto ethyl esters **8** into 6-alkyl-pipercolates (Figure 6). The esters were added to the *A. nidulans* culture and after growth for 4-5 days, formation of 6-alkyl-pipercolates was monitored by LCMS. New pipercolate compounds were extracted and purified from culture (Figure S11), and were structurally characterized by NMR (Figure 6).

We were able to obtain several 6-alkyl pipercolates by fermentation, with yields ranging from 1-5 mg/L. While the titers of molecules shown in Figure 6 are modest, we suspect the limiting substrate in *A. nidulans* is *O*-acetyl-L-homoserine **9**. Production of **9** completely relies on a single copy of HAT gene encoded in the genome. Increasing the pool of **9** by overexpressing additional copies of HAT gene may significantly improve the titer of the products.

The abilities of the different esters to be transformed into pipercolate generally match to what was observed *in vitro* (Figure 5), with several notable exceptions attributed to the removal of the ethyl ester *in cellulo*. For  $\beta$ -keto esters (**8e-g**) that can be consumed by CndF *in vitro* to give enamine esters, 6-substituted pipercolates **22**, **23**, and **24** were synthesized, respectively (Tables S9-S11, Figures S41-S58). Interestingly, the biosynthesis of **23** in the presence of the *tert*-butyl containing **8f** suggests that once the ethyl ester is hydrolyzed, the corresponding adduct can cyclize into the Schiff base. While **8i** was not transformed by CndF *in vitro*, we can detect and

purify the corresponding 6-cyclopentane-pipercolate **25** from *A. nidulans* (Table S12, Figures S59-S64). This suggests that once the ethyl ester is hydrolyzed to the carboxylate, the active site of CndF can accommodate the bulky  $R_1$  substituent. However, larger  $R_1$  groups such as the phenyl group (**8o**) still cannot be recognized by CndF to make 6-phenyl-pipercolate. The formation of **22-25** also shows the SDR CndE can tolerate substantially larger substituents at C6 in performing imine reduction. The stereochemical configurations of these compounds have all been confirmed by NOESY analysis. There are no endogenous reductases in *A. nidulans* that can intercept the imine intermediates generated by CndF to produce diastereoisomers. Therefore, coupling CndF with a promiscuous *R*-specific imine reductase can potentially lead to the production of (2*S*, 6*R*)-6-alkyl pipercolate.<sup>58</sup>

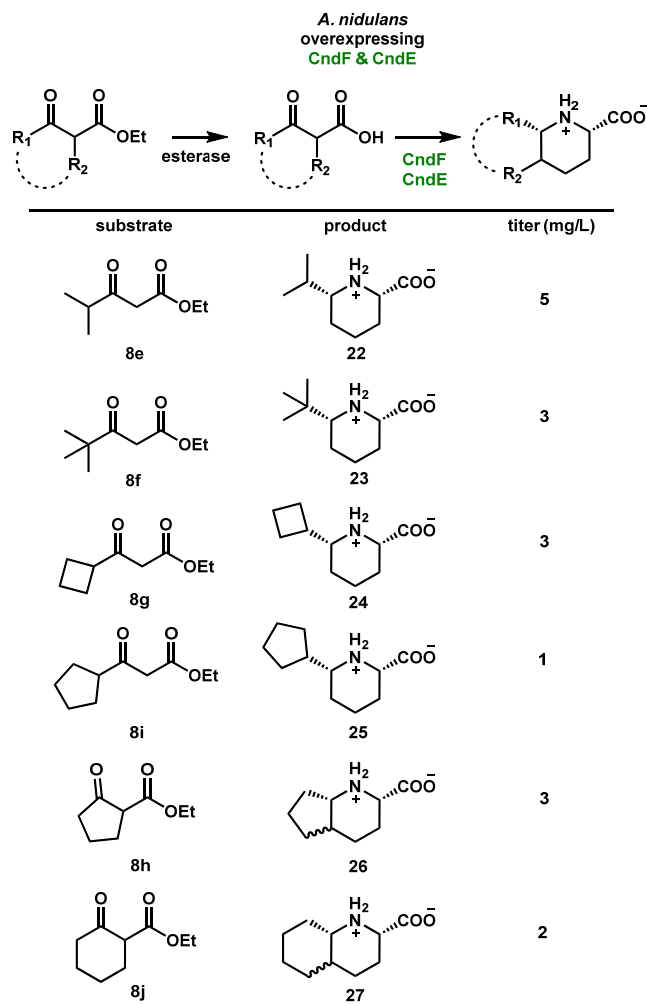


**Figure 6.** In vivo biosynthesis of substituted pipercolates.

In addition to **1**, we observed production of enamine **14** in large amounts from *A. nidulans* when **8a** is supplied (Figure S12A). When  $R_1$  substituent is bulkier as in **8b** or **8c**, enamine formation becomes barely detectable (Figure S12A). We reasoned that the ethyl esters **8** is subjected to competing hydrolysis by esterases and C-C bond formation by CndF in *A. nidulans*. When  $R_1$  substituent is small as in **8a**, the rates of hydrolysis and  $\gamma$ -substitution are comparable, which results in the formation of both enamine ester **14** and pipercolate **1**. When  $R_1$  substituent becomes bulkier, the C-C bond formation rate

of ethyl ester is slower than that of ester hydrolysis, leading to the formation of nearly all 6-alkyl pipercolate products (Figure S12B).

Lastly, bicyclic **26** and **27** can be produced from ethyl 2-oxocyclopentanecarboxylate **8h** and ethyl 2-oxocyclohexanecarboxylate **8j**, respectively (Tables S13–15 and Figures S65–S82). Similar to **8i**, we did not observe enamine formation for **8j** *in vitro*, but **27** was detected and isolated *in vivo* as a result of ethyl ester hydrolysis. Both **8h** and **8j** were supplied as racemic mixtures due to facile racemization at the C $\alpha$  position. From biotransformation, we observed a pair of diastereomers for both **26** and **27** at nearly 1:1 ratios (Figure S11). **8h** was converted to octahydro-1*H*-cyclopenta[b]pyridine-2-carboxylic acid **26<sub>cis</sub>** and **26<sub>trans</sub>** at 1:1 ratio, although we were only able to structurally characterize **26<sub>cis</sub>** by NMR due to separation difficulties associated with **26<sub>trans</sub>**. Octahydro-1*H*-cyclopenta[b]pyridine-6-carboxylic acid, an analogue of **26**, is a conformationally restricted  $\gamma$ -aminobutyric acid (GABA) analogue.<sup>59</sup> Considering the noted neuroactivity of pipercolates,<sup>60</sup> we speculate that **26<sub>cis</sub>** and **26<sub>trans</sub>** could be useful as conformationally restricted analogues of L-pipercolates.<sup>60–61</sup> Similar to **8h**, **8j** is presumably hydrolyzed by *A. nidulans* esterase to yield racemic  $\beta$ -keto acids, which were converted to a pair of cyclic imines at 1:1 ratio by CndF. CndE can reduce the imines to either the *cis*-azadecalin **27<sub>cis</sub>** or *trans*-azadecalin **27<sub>trans</sub>**, as confirmed by NMR analysis. Previous studies showed that racemic **27** produced by hydrogenation of quinoline-2-carboxylic acid is a potent inhibitor of Angiotensin I converting enzyme.<sup>62</sup> Coupling of CndF and CndE offers a biocatalytic route to produce decahydroquinoline-2-carboxylic acids. We reason that scrambling of the C5 stereocenter in **26** and **27** may occur as a result of  $\beta$ -decarboxylation after the C–C bond formation step, during which formation of an enol intermediate effectively scrambles the previously established C5 stereocenter.

## SUMMARY

Abundant genome sequences have provided unprecedented opportunities to uncover new enzyme reactivities from natural product biosynthetic pathways. In this work, we identified a succinct, two-step pathway to synthesize the noncanonical amino acid (2*S*, 6*S*)-6-methyl pipercolate **1**. The first step is a C $\gamma$ –C $\delta$  bond substitution reaction between *O*-acetyl L-homoserine and acetoacetate, catalyzed by a PLP-dependent enzyme. The second step is stereoselective Schiff base reduction catalyzed by an imine reductase. The substrate tolerances exhibited by the two enzymes enabled biocatalytic synthesis of a panel of 6-alkyl pipercolate derivatives. In addition, CndF can accept  $\beta$ -keto ethyl esters to generate enamine containing pipercolate molecules. CndF displays new catalytic mechanism in catalyzing  $\gamma$ -substitution and C–C bond formation using the PLP cofactor. CndF therefore represents an attractive starting point for biocatalyst engineering, as well interfacing with other enzymes or synthetic methodology to further elaborate the product structures.

## ASSOCIATED CONTENT

## AUTHOR INFORMATION

### Corresponding Author

\*Yi Tang yitang@ucla.edu

### Notes

The authors declare no conflict of interest.

## ACKNOWLEDGMENT

This work was supported by the NIH 1R35GM118056 to Y.T. Structural characterization by NMR is based upon work supported by the National Science Foundation under equipment grant no. CHE-1048804. We thank Drs. Y. Hai and W. Cheng for helpful discussions.

## REFERENCES

- Walsh, C. T.; O'Brien, R. V.; Khosla, C., Nonproteinogenic Amino Acid Building Blocks for Nonribosomal Peptide and Hybrid Polyketide Scaffolds. *Angew. Chem. Int. Ed.* **2013**, *52*, 7098–7124.
- Hedges, J. B.; Ryan, K. S., Biosynthetic Pathways to Nonproteinogenic  $\alpha$ -Amino Acids. *Chem. Rev.* **2019**.
- Blaskovich, M. A. T., Unusual Amino Acids in Medicinal Chemistry. *J. Med. Chem.* **2016**, *59*, 10807–10836.
- Baumann, M.; Baxendale, I. R., An overview of the synthetic routes to the best selling drugs containing 6-membered heterocycles. *Beilstein J. Org. Chem.* **2013**, *9*, 2265–2319.
- White, C. J.; Yudin, A. K., Contemporary strategies for peptide macrocyclization. *Nat. Chem.* **2011**, *3*, 509–524.
- Liu, C. C.; Schultz, P. G., Adding New Chemistries to the Genetic Code. *Annual Review of Biochemistry* **2010**, *79*, 413–444.
- Lerchen, A.; Knecht, T.; Daniluc, C. G.; Glorius, F., Unnatural Amino Acid Synthesis Enabled by the Regioselective Cobalt(III)-Catalyzed Intermolecular Carboamination of Alkenes. *Angew. Chem. Int. Ed.* **2016**, *55*, 15166–15170.
- Kiss, L.; Fülöp, F., Synthesis of Carbocyclic and Heterocyclic  $\beta$ -Aminocarboxylic Acids. *Chem. Rev.* **2014**, *114*, 1116–1169.
- Turner, N. J., Ammonia lyases and aminomutases as biocatalysts for the synthesis of  $\alpha$ -amino and  $\beta$ -amino acids. *Curr. Opin. Chem. Biol.* **2011**, *15*, 234–240.
- Steinreiber, J.; Fesko, K.; Reisinger, C.; Schürmann, M.; van Assema, F.; Wolberg, M.; Mink, D.; Griengl, H., Threonine aldolases—an emerging tool for organic synthesis. *Tetrahedron* **2007**, *63*, 918–926.
- Wu, B.; Szymański, W.; Heberling, M. M.; Feringa, B. L.; Janssen, D. B., Aminomutases: mechanistic diversity, biotechnological applications and future perspectives. *Trends Biotechnol.* **2011**, *29*, 352–362.
- Bornscheuer, U. T.; Huisman, G. W.; Kazlauskas, R. J.; Lutz, S.; Moore, J. C.; Robins, K., Engineering the third wave of biocatalysis. *Nature* **2012**, *485*, 185–194.
- Zwick, C. R.; Renata, H., Remote C–H Hydroxylation by an  $\alpha$ -Ketoglutarate-Dependent Dioxygenase Enables Efficient Chemoenzymatic Synthesis of Manzacidin C and Proline Analogs. *J. Am. Chem. Soc.* **2018**, *140*, 1165–1169.
- Neugebauer, M. E.; Sumida, K. H.; Pelton, J. G.; McMurry, J. L.; Marchand, J. A.; Chang, M. C. Y., A family of radical halogenases for the engineering of amino-acid-based products. *Nat. Chem. Biol.* **2019**, *15*, 1009–1016.
- Marchand, J. A.; Neugebauer, M. E.; Ing, M. C.; Lin, C. I.; Pelton, J. G.; Chang, M. C. Y., Discovery of a pathway for terminal-alkyne amino acid biosynthesis. *Nature* **2019**, *567*, 420–424.
- Lukat, P.; Katsuyama, Y.; Wenzel, S.; Binz, T.; König, C.; Blankenfeldt, W.; Brönstrup, M.; Müller, R., Biosynthesis of methyl-proline containing griselimycins, natural products with anti-tuberculosis activity. *Chem. Sci.* **2017**, *8*, 7521–7527.
- Wilson, K. P.; Yamashita, M. M.; Sintchak, M. D.; Rotstein, S. H.; Murcko, M. A.; Boger, J.; Thomson, J. A.; Fitzgibbon, M. J.; Black, J. R.; Navia, M. A., Comparative X-ray structures of the major binding protein for the immunosuppressant FK506 (tacrolimus) in unliganded form and in complex with FK506 and rapamycin. *Acta Crystallogr. D* **1995**, *51*, 511–521.
- Graziani, E. I., Recent advances in the chemistry, biosynthesis and pharmacology of rapamycin analogs. *Nat. Prod. Rep.* **2009**, *26*, 602–609.
- Barluenga, J.; Fernández, M. A.; Aznar, F.; Valdés, C., Catalytic imino-Diels–Alder reactions of 2-aminodienes: a simple entry into structurally diverse pipercolic acid derivatives. *Tetrahedron Lett.* **2002**, *43*, 8159–8163.
- Kano, T.; Kumano, T.; Sakamoto, R.; Maruoka, K., Catalytic asymmetric synthesis of cyclic amino acids and alkaloid derivatives:



- application to (+)-dihydropinidine and Selfotel synthesis. *Chem. Sci.* **2010**, *1*, 499-501.
21. Rutjes, F. P. J. T.; Schoemaker, H. E., Ruthenium-catalyzed ring closing olefin metathesis of non-natural  $\alpha$ -amino acids. *Tetrahedron Lett.* **1997**, *38*, 677-680.
  22. Davis, F. A.; Zhang, H.; Lee, S. H., Masked Oxo Sulfinimines (N-Sulfinyl Imines) in the Asymmetric Synthesis of Proline and Pípecolic Acid Derivatives. *Org. Lett.* **2001**, *3*, 759-762.
  23. Pérez-García, F.; Max Risse, J.; Friehs, K.; Wendisch, V. F., Fermentative production of L-pípecolic acid from glucose and alternative carbon sources. *Biotechnol. J.* **2017**, *12*, 1600646.
  24. Gatto, G. J.; Boyne, M. T.; Kelleher, N. L.; Walsh, C. T., Biosynthesis of Pípecolic Acid by RapL, a Lysine Cyclodeaminase Encoded in the Rapamycin Gene Cluster. *J. Am. Chem. Soc.* **2006**, *128*, 3838-3847.
  25. Hartmann, M.; Kim, D.; Bernsdorff, F.; Ajami-Rashidi, Z.; Scholten, N.; Schreiber, S.; Zeier, T.; Schuck, S.; Reichel-Deland, V.; Zeier, J., Biochemical Principles and Functional Aspects of Pípecolic Acid Biosynthesis in Plant Immunity. *Plant Physiol.* **2017**, *174*, 124.
  26. Wickwire, B. M.; Harris, C. M.; Harris, T. M.; Broquist, H. P., Pípecolic acid biosynthesis in Rhizoctonia leguminicola. I. The lysine saccharopine, delta 1-piperidine-6-carboxylic acid pathway. *J. Biol. Chem.* **1990**, *265*, 14742-7.
  27. Li, L.; Tang, M.-C.; Tang, S.; Gao, S.; Soliman, S.; Hang, L.; Xu, W.; Ye, T.; Watanabe, K.; Tang, Y., Genome Mining and Assembly-Line Biosynthesis of the UCS1025A Pyrrolizidinone Family of Fungal Alkaloids. *J. Am. Chem. Soc.* **2018**, *140*, 2067-2071.
  28. Luesch, H.; Hoffmann, D.; Hevel, J. M.; Becker, J. E.; Golakoti, T.; Moore, R. E., Biosynthesis of 4-Methylproline in Cyanobacteria: Cloning of nosE and nosF Genes and Biochemical Characterization of the Encoded Dehydrogenase and Reductase Activities. *J. Org. Chem.* **2003**, *68*, 83-91.
  29. Yee, D. A.; Kakule, T. B.; Cheng, W.; Chen, M.; Chong, C. T. Y.; Hai, Y.; Hang, L. F.; Hung, Y.-S.; Liu, N.; Ohashi, M.; Okorafor, I. C.; Song, Y.; Tang, M.; Zhang, Z.; Tang, Y., Genome Mining of Alkaloidal Terpenoids from a Hybrid Terpene and Nonribosomal Peptide Biosynthetic Pathway. *J. Am. Chem. Soc.* **2020**, *142*, 710-714.
  30. Tsuda, M.; Kasai, Y.; Komatsu, K.; Sone, T.; Tanaka, M.; Mikami, Y.; Kobayashi, J. i., Citrinadin A, a Novel Pentacyclic Alkaloid from Marine-Derived Fungus Penicillium citrinum. *Org. Lett.* **2004**, *6*, 3087-3089.
  31. Mugishima, T.; Tsuda, M.; Kasai, Y.; Ishiyama, H.; Fukushi, E.; Kawabata, J.; Watanabe, M.; Akao, K.; Kobayashi, J. i., Absolute Stereochemistry of Citrinadins A and B from Marine-Derived Fungus. *J. Org. Chem.* **2005**, *70*, 9430-9435.
  32. Kushida, N.; Watanabe, N.; Okuda, T.; Yokoyama, F.; Gyobu, Y.; Yaguchi, T., PF1270A, B and C, Novel Histamine H3 Receptor Ligands Produced by Penicillium waksmanii PF1270. *J. Antibiot.* **2007**, *60*, 667-673.
  33. Bian, Z.; Marvin, C. C.; Martin, S. F., Enantioselective Total Synthesis of (-)-Citrinadin A and Revision of Its Stereochemical Structure. *J. Am. Chem. Soc.* **2013**, *135*, 10886-10889.
  34. Kong, K.; Enquist, J. A.; McCallum, M. E.; Smith, G. M.; Matsumaru, T.; Menhaji-Klotz, E.; Wood, J. L., An Enantioselective Total Synthesis and Stereochemical Revision of (+)-Citrinadin B. *J. Am. Chem. Soc.* **2013**, *135*, 10890-10893.
  35. Guerrero, C. A.; Sorensen, E. J., Concise, Stereocontrolled Synthesis of the Citrinadin B Core Architecture. *Org. Lett.* **2011**, *13*, 5164-5167.
  36. Mercado-Marin, E. V.; Garcia-Reynaga, P.; Romminger, S.; Pimenta, E. F.; Romney, D. K.; Lodewyk, M. W.; Williams, D. E.; Andersen, R. J.; Miller, S. J.; Tantillo, D. J.; Berlinck, R. G. S.; Sarpong, R., Total synthesis and isolation of citrinalin and cyclopiamine congeners. *Nature* **2014**, *509*, 318-324.
  37. Klas, K. R.; Kato, H.; Frisvad, J. C.; Yu, F.; Newmister, S. A.; Fraley, A. E.; Sherman, D. H.; Tsukamoto, S.; Williams, Robert M., Structural and stereochemical diversity in prenylated indole alkaloids containing the bicyclo[2.2.2]diazaoctane ring system from marine and terrestrial fungi. *Nat. Prod. Rep.* **2018**, *35*, 532-558.
  38. Dan, Q.; Newmister, S. A.; Klas, K. R.; Fraley, A. E.; McAfoos, T. J.; Somoza, A. D.; Sunderhaus, J. D.; Ye, Y.; Shende, V. V.; Yu, F.; Sanders, J. N.; Brown, W. C.; Zhao, L.; Paton, R. S.; Houk, K. N.; Smith, J. L.; Sherman, D. H.; Williams, R. M., Fungal indole alkaloid biogenesis through evolution of a bifunctional reductase/Diels-Alderase. *Nat. Chem.* **2019**, *11*, 972-980.
  39. Fraley, A. E.; Caddell Haatveit, K.; Ye, Y.; Kelly, S. P.; Newmister, S. A.; Yu, F.; Williams, R. M.; Smith, J. L.; Houk, K. N.; Sherman, D. H., Molecular Basis for Spirocyclic Formation in the Paraherquamide Biosynthetic Pathway. *J. Am. Chem. Soc.* **2020**, *142*, 2244-2252.
  40. Stegink, L. D.; Coon, M. J., Stereospecificity and Other Properties of Highly Purified  $\beta$ -Hydroxy- $\beta$ -methylglutaryl Coenzyme A Cleavage Enzyme from Bovine Liver. *J. Biol. Chem.* **1968**, *243*, 5272-5279.
  41. Eliot, A. C.; Kirsch, J. F., Pyridoxal Phosphate Enzymes: Mechanistic, Structural, and Evolutionary Considerations. *Annual Review of Biochemistry* **2004**, *73*, 383-415.
  42. Du, Y.-L.; Ryan, K. S., Pyridoxal phosphate-dependent reactions in the biosynthesis of natural products. *Nat. Prod. Rep.* **2019**, *36*, 430-457.
  43. Wiebers, J. L.; Garner, H. R., Acyl Derivatives of Homoserine as Substrates for Homocysteine Synthesis in Neurospora crassa, Yeast, and Escherichia coli. *J. Biol. Chem.* **1967**, *242*, 5644-5649.
  44. Brzovic, P.; Holbrook, E. L.; Greene, R. C.; Dunn, M. F., Reaction mechanism of Escherichia coli cystathionine  $\gamma$ -synthase: direct evidence for a pyridoxamine derivative of vinylglyoxylate as a key intermediate in pyridoxal phosphate dependent  $\gamma$ -elimination and  $\gamma$ -amino-replacement reactions. *Biochemistry* **1990**, *29*, 442-451.
  45. Zhang, Z.; Jamieson, C. S.; Zhao, Y.-L.; Li, D.; Ohashi, M.; Houk, K. N.; Tang, Y., Enzyme-Catalyzed Inverse-Electron Demand Diels-Alder Reaction in the Biosynthesis of Antifungal Illicolins H. *J. Am. Chem. Soc.* **2019**, *141*, 5659-5663.
  46. Borthwick, A. D., 2,5-Diketopiperazines: Synthesis, Reactions, Medicinal Chemistry, and Bioactive Natural Products. *Chem. Rev.* **2012**, *112*, 3641-3716.
  47. Singh, S.; Brocker, C.; Koppaka, V.; Chen, Y.; Jackson, B. C.; Matsumoto, A.; Thompson, D. C.; Vasiliou, V., Aldehyde dehydrogenases in cellular responses to oxidative/electrophilic stress. *Free Radical Biol. Med.* **2013**, *56*, 89-101.
  48. Bhushan, R.; Brückner, H., Marfey's reagent for chiral amino acid analysis: A review. *Amino Acids* **2004**, *27*, 231-247.
  49. Griswold, W. R.; Toney, M. D., Role of the Pyridine Nitrogen in Pyridoxal 5'-Phosphate Catalysis: Activity of Three Classes of PLP Enzymes Reconstituted with Deazapyridoxal 5'-Phosphate. *J. Am. Chem. Soc.* **2011**, *133*, 14823-14830.
  50. Metzler, D. E.; Ikawa, M.; Snell, E. E., A General Mechanism for Vitamin B6-catalyzed Reactions I. *J. Am. Chem. Soc.* **1954**, *76*, 648-652.
  51. Walsh, C. T., Biologically generated carbon dioxide: nature's versatile chemical strategies for carboxy lyases. *Nat. Prod. Rep.* **2020**, *37*, 100-135.
  52. Han, L.; Vuksanovic, N.; Oehm, S. A.; Fenske, T. G.; Schwabacher, A. W.; Silvaggi, N. R., Streptomyces wadayamensis MppP is a PLP-Dependent Oxidase, Not an Oxygenase. *Biochemistry* **2018**, *57*, 3252-3264.
  53. Faulkner, J. R.; Hussaini, S. R.; Blankenship, J. D.; Pal, S.; Branan, B. M.; Grossman, R. B.; Schardl, C. L., On the Sequence of Bond Formation in Loline Alkaloid Biosynthesis. *ChemBioChem* **2006**, *7*, 1078-1088.
  54. Ye, Y.; Minami, A.; Igarashi, Y.; Izumikawa, M.; Umemura, M.; Nagano, N.; Machida, M.; Kawahara, T.; Shin-ya, K.; Gomi, K.; Oikawa, H., Unveiling the Biosynthetic Pathway of the Ribosomally Synthesized and Post-translationally Modified Peptide Ustiloxin B in Filamentous Fungi. *Angew. Chem. Int. Ed.* **2016**, *55*, 8072-8075.
  55. Hofmann, D.; Kosower, E. M.; Wallenfels, K., The Effect of Solvent on Spectra. VII. The "Methyl Effect" in the Spectra of Dihydropyridines. *J. Am. Chem. Soc.* **1961**, *83*, 3314-3319.
  56. Wang, E.; Walsh, C., Suicide substrates for the alanine racemase of Escherichia coli B. *Biochemistry* **1978**, *17*, 1313-1321.
  57. Mayordomo, I.; Rande-Gil, F.; Prieto, J. A., Isolation, Purification, and Characterization of a Cold-Active Lipase from Aspergillus nidulans. *J. Agric. Food. Chem.* **2000**, *48*, 105-109.

58. Hussain, S.; Leipold, F.; Man, H.; Wells, E.; France, S. P.; Mulholland, K. R.; Grogan, G.; Turner, N. J., An (R)-Imine Reductase Biocatalyst for the Asymmetric Reduction of Cyclic Imines. *ChemCatChem* **2015**, *7*, 579-583.
59. Melnykov, K. P.; Volochnyuk, D. M.; Ryabukhin, S. V.; Rusanov, E. B.; Grygorenko, O. O., A conformationally restricted GABA analogue based on octahydro-1H-cyclopenta[b]pyridine scaffold. *Amino Acids* **2019**, *51*, 255-261.
60. Hallen, A.; Jamie, J. F.; Cooper, A. J. L., Lysine metabolism in mammalian brain: an update on the importance of recent discoveries. *Amino Acids* **2013**, *45*, 1249-1272.
61. Anna, J.; Rafal, K., Conformationally Restricted Peptides as Tools in Opioid Receptor Studies. *Curr. Med. Chem.* **2005**, *12*, 471-481.
62. Wright, G. C.; White, R. E. Decahydroquinoline-2-carboxylic acid compounds. U.S. Patent US4291163A, **1981**.

TOC Figure

